Synthesis, Structural and Dielectric Studies on SrBi2-xGdxNb2O9 Lead Free Ceramics

Nitchal Kiran Jaladi (kiran.nischal@gmail.com)
VFSTR University
K. Sambasiva Rao
Andhra University
Haileeyesus Workineh
Bahir Dar University
J. Anindhya Kiran
Vignan Institute of Technology and Science
S. Nagamani
Vignan's Foundation for Science Technology and Research

Research Article

Keywords: Relaxor ferroelectric, X-ray diffraction, Dielectric studies, Diffuseness parameter

Posted Date: October 16th, 2020

DOI: https://doi.org/10.21203/rs.3.rs-91046/v1

Abstract

In this manuscript, the structural and dielectric properties of Gadolinium (Gd^{3+}) substituted at Bi-site of $SrBi_{2-x}Gd_xNb_2O_9$ (x= 0.0, 0.4, 0.6 and 0.8) prepared by using solid state reaction are studied. XRD analysis revealed the formation of single phase with orthorhombic structure in SBN and Gadolinium modified SBN. It is found that cell parameters and volume were decreased with increase of Gd^{3+} ion concentration in SBN. SEM analysis revealed that the samples possess well defined needle shaped grains. The grain size of SBN was hindered by the presence of Gd^{3+} ion at Bi-site. The growth of single phase layered perovskite structure was confirmed from FTIR and Raman spectroscopy. The dielectric properties of Gd^{3+} ion doped SBN ceramics are studied as a function of frequency (50Hz-1MHz) from room temperature to 500ºC. It is observed that phase transition temperature (T_c) decreased from 430ºC to 330ºC with increase of frequency due to incorporation of Gd^{3+} ion in SBN. The broadness of peaks and decrease in T_c indicate the transition from a normal ferroelectric to ferroelectric-relaxor type. The study on variation of tanδ with temperature at different frequencies indicates that tanδ has larger values at higher temperatures. Further, the diffuseness parameter (γ) has been computed for all the compositions.

1. Introduction

$SrBi_2Nb_2O_9$ (SBN) has been regarded as a promising ferroelectric material due to the attributes of low dielectric constant, high mechanical quality factor, low electromechanical coupling coefficient and an excellent electro-optic property. At present, bismuth layered structure ferroelectrics (BLSF) such as $SrBi_2Nb_2O_9$ (SBN) and $SrBi_2Ta_2O_9$ (SBT) are under good investigation as they have most promising device applications such as Non-Volatile Random Access Memories (NVRAM), sensors, actuators, fine tolerance oscillators and high capacitance capacitors [1-10].When compared to $Pb(Zr,Ti)O_3$ (PZT), a non-layered ferroelectric, SBN has several advantages such as fatigue free, lead free, minimum operating voltages, a high mechanical quality factor and low temperature coefficient of resonance frequency [11,12]. SBN material of $(Bi_2O_2)^{2+}$ interleaved with pseudo perovskite blocks $(A_{n-1}B_nO_{3n+1})^{2+}$ are sensitive to doping with various elements [13] and bismuth layer influences the structural, electrical and ferroelectric properties of the materials [14]. Sintering conditions and doping at different sites will lead to the change in the physical properties of the materials. As per our literature survey, rare earth group elements (or) lanthanides with incomplete 4f shell doped interleaved structures find important technical applications in the field of electronics and optoelectronics. The studies based on perovskite structure such as RMnO (R= Y, Dy, Ho, Tb, Yb etc.,) have exhibited multiferroic properties [15-19]. Lanthanides doped SBN compound demonstrated rise in the dielectric loss due to annihilation of bismuth during sintering process. In view of this, it is desirable to dope SBN with rare earth ions [20-22]. Hence, an attempt is made to study the modified properties of SBN doping gadolinium at Bi- site of it. In the present study, sintering conditions in processing of SBN and gadolinium doped SBN have been established and studied the effect of gadolinium on the structure, microstructure and dielectric properties.

2. Experimental

Solid state reaction method was used to prepare the ceramic compositions, SrBi2Nb2O9 (SBN), SrBi1.6Gd0.4Nb2O9 (SB0.4GN), SrBi1.4Gd0.6Nb2O9 (SB0.6GN) and SrBi1.2Gd0.8Nb2O9 (SB0.8GN), mainly using of highly pure powders of oxides and carbonate. The powders upon mixing were subjected to calcination at 800˚C for 2hr thrice to enhance the homogeneity of the materials. The calcined materials were sintered in the temperature range of 1120□C-1150□C. The either sides of pellets were electroplated using silver paste. X-ray diffraction data were collected for these samples using Cu kα radiation in the range (10˚≤2θ≤90˚). Scanning electron microscope (SEM) measurements are performed using vega3 tescan. Fourier Trasform Infrared (FTIR) spectra of samples using KBr were recorded between 3,500-400 cm-1 using YLS-QC-WQP-004. The Raman spectra were recorded by Raman microscope using 785 nm solid state laser beams. Dielectric measurements carried out in the temperature and frequency range (RT -500oC) and (50Hz – 1MHz) respectively using a HP4284A impedance analyser.

3. Results And Discussion

3.1 Density

The optimum value of sintering temperature for maximum sintered density has been achieved from density versus composition response, over a wide range of temperature (1120□C-1150□C) as shown in fig. 1. The maximum density for the studied samples has been obtained at 1120□C for 2 hours.

3.2 X-ray Diffraction Analysis

Fig. 2 shows XRD analysis of SBN & SBGN materials obtained using RigakuMiniflex 300/600. A standard computer programme of POWD [23] is used to index the peaks and estimation of lattice parameters. The intensity peaks of X-ray diffractrograms show the formation of BLSF with the single phase orthorhombic structure. The substitution of gadolinium at Bi-site of SBN has resulted in a small shift in the position and intensity in XRD spectra of the studied ceramic samples. This is due to the substitution of gadolinium in SBN, which in turn led to a variation in the values of lattice parameters. From the gadolinium substitution at Bi-site of SBN, lattice parameter values and cell volume has been found to decrease, shown in fig. 3. The decrease in the lattice parameters can be ascribed to the substitution of the larger radius of Bi^{3+} ion (1.020 Å) compared to that Gd^{3+} ion (0.938 Å) [24, 25]. Further, the orthorhombic distortion values also are identified to decrease from SBN values. The structural parameters determined from XRD study are given in table.1.

3.3 Microstructure- SEM

Fig. 4 shows the microstructure in the studied materials obtained from SEM. The plate like morphology observed from SEM is symbolic of characteristic Aurivillius phase of ceramics. [26]. From the figure it is clear that SEM images exhibits microstructure with large needle shaped grains with induced porosity and inhomogeneous distribution upon gadolinium doping SBN as shown in the fig. 3 (b-d). The porosity is

induced in these materials corresponding to the measured density in the ceramic samples. Substitution of gadolinium in SBN inhibits the grain growth and is evident from table. 2

3.4 FTIR and Raman studies

Powders of SBN and SBGN calcined at 800°C have been taken for FTIR spectra and the spectra are shown in the fig. 5(a). FTIR mode observed at 419 cm^{-1} corresponds to the Nb-O bending vibration, and mode at 501cm^{-1} corresponds to Bi-O vibration of α-Bi_2O_3. The Raman spectroscopy is a very effective and sensitive for identifying phase purity of multi component oxide material. Raman Spectra obtained at room temperature on SBN and SBGN calcined powders are shown in fig. 5(b). As the gadolinium concentration in SBN increases it is noticed that there is no change in the phonon modes corresponding to tilting of NbO_6 octahedral. A sharp Raman mode was observed at 174 cm^{-1} in the Raman spectra. Symmetric stretch of NbO_6 octahedral has been observed at 836cm^{-1} as a frequency band. Thus from Raman study, formation of NbO_6 octahedral is confirmed.

3.5 Dielectric studies

Fig. 6(a) and fig. 6(b) shows the variation of dielectric permittivity versus temperature (RT-500˚C) at selected frequencies (450Hz, 1KHz, 5KHz, 10KHz and 1MHz) for SBN and gadolinium modified SBN materials respectively. It has been observed a transition from Ferroelectric to Para electric phase in all the studied materials. The value of transition temperature (T_c) in SBN has been found at 430°C, noticed to be close agreement with literature value [27-28]. The transition temperatures (T_c) of the studied ceramics are found to lie in the temperature range 430°C-330°C. Predominantly, the transition temperature of ferroelectric materials depends on the polarizability of them. The lower transition temperature in the Gd^{3+} ion substituted sample of $SB_{0.4}GN$ (T_c=350°C) may be due to size dependent electronic polarization and decreased tetragonal strain in the sample [14, 29]. The values of T_c are further reduced to 340°C and 330°C in $SB_{0.6}GN$ and $SB_{0.8}GN$ respectively compared to SBN. The response of dielectric permittivity with temperature at different frequencies showed a broad response. The broadness is found to increase with increase in frequency. This suggests that the present materials are of relaxor type. The room temperature dielectric constant of SBN increased from 127 to 168 in $SB_{0.4}GN$. Further increase in gadolinium concentration, dielectric constant value decreased in both $SB_{0.6}GN$ and $SB_{0.8}GN$. The ceramic materials of $SB_{0.6}GN$ and $SB_{0.8}GN$ exhibited a similar behaviour to that of $SB_{0.4}GN$ along with SBN from the above study. The typical variation of dielectric constant with temperature for SBN and $SB_{0.4}GN$ at different frequencies is shown in fig. 6(a) and fig. 6(b).

Fig. 7(a) and fig. 7(b) shows the typical dielectric constant versus frequency (100Hz - 1MHz) at different temperatures. The variation of permittivity with increasing frequency exhibited the relaxor behaviour. This is typical of thermally activated Debye relaxation in these frequency regions. The increase in dielectric permittivity at higher temperature can be assigned to increase in conductivity [29, 30] due to the mobile charge carriers raised from the formation of oxygen vacancies arising from volatilization of

bismuth during the sintering [31, 32]. The substitution of Gd^{3+} ion at Bi-site of SBN not only restrains the bismuth losses, caused a decrease in conduction phenomenon, therefore dielectric permittivity decreased [33]. Meanwhile, small polarization of Gd^{3+} ion in comparison with Bi^{3+} ion may be the reason for small [34]. A similar behaviour has been observed in both $SB_{0.6}GN$ and $SB_{0.8}GN$ ceramic materials. The flattening of dielectric permittivity and low dielectric loss are desirable features to suit Non-volatile Fe RAM applications [25].

Fig. 8 shows typical dielectric loss measured at different frequencies (100Hz - 1MHz) as a function of selected temperatures of $SB_{0.4}GN$ material. The decrease in dielectric loss with increase in frequency in $SB_{0.4}GN$ is due to space charge and domain wall relaxation [35]. A similar trend has been observed in both $SB_{0.6}GN$ and $SB_{0.8}GN$ ceramics.

3.6 Diffusivity Parameter

The modified Curie-Weiss law is employed to understand diffuse phase transition and relaxation behaviour in the material. The modified Curie–Weiss law was given in the equation (1)

$$1/\varepsilon - 1/\acute{\varepsilon}_{max} = (T - T_m)^{\gamma}/C \qquad (1)$$

Where, ε'_{max} is maximum permittivity at T_m, ε' is the permittivity, T is temperature above T_m (in the paraelectric region), C is a constant and γ is the diffuseness parameter representing the degree of dielectric relaxation ($1 \leq \gamma \leq 2$). For a normal ferroelectric γ = 1. For a completely disordered ferroelectric, γ = 2 [36-38]. When 1 < γ < 2, the material is called relaxor ferroelectric. Fig.9 shows a typical variation of ln $[(\varepsilon'_{max}/\varepsilon') - 1]$ versus ln $(T - T_m)$ for the $SB_{0.4}GN$ sample at 1MHz taking modified Curie- Weiss law, linearly fitting the experimental data. The diffuseness parameter γ was found to be 1.37 in $SB_{0.4}GN$. This shows diffuse nature of phase transition in $SB_{0.4}GN$. The diffuse phase transition (DPT) can mainly be due to substitution of cation-host with some elements having different ionic radii [39, 40]. Long et al. [41] considering the structure of $Na_{0.5}Nd_xBi_{2.5-x}Nb_2O_9$ (NNBN) (x = 0.1, 0.2, 0.3 and 0.5) suggested that Nd^{3+} ions occupied Na-site in NNBN and are diffused into the $(Bi_2O_2)^{2+}$ slabs. In view of the above, it can be concluded that the distortion induced by the Gd^{3+} ion modification could be a possible reason for the diffuseness behaviour in the present ceramic materials [42-43]. A similar behaviour has been observed in case of $SB_{0.6}GN$ and $SB_{0.8}GN$ compositions along with SBN, given in table 4. The relaxor ferroelectrics with diffuse phase transitions (DPT) had found applications in different devices such as piezoelectric actuators, multilayer capacitors, medical imaging devices, non-volatile memories, pyroelectric detectors and microwave tuneable applications [44-46].

4. Conclusions

Polycrystalline $SrBi_{2-x}Gd_xNb_2O_9$ (x = 0.0, 0.4, 0.6 and 0.8) ceramic compositions were prepared by the conventional high temperature solid–state reaction method. High dense, about 93-96% to that of theoretical value ceramic samples are obtained by establishing sintering conditions. SBN and SBGN have been indexed to be single phase with orthorhombic structure from XRD analysis. Substitution of Gd in Bi-site in SBN not only reduced lattice parameters but also cell volume. FTIR shows the distortion of NbO_6 octahedral with Gd doping. The appearance of sharp Raman mode at 174 cm^{-1} high dielectric constant and low dielectric loss confirms the fabrication of good quality ceramics suitable for Ferroelectric Random Access memory (Fe RAM) devices. Substitution of Gd in SBN decreased T_c from 430^oC-330^oC. The dielectric constant versus temperature response at different frequencies showed a broad response, suggesting that the present samples are of relaxor type. The diffusivity parameter is found to lie in between 1 to 2, which means that the materials belong to relaxor ferroelectrics remain and suitable for many device applications.

References

[1] B. H. Park, B. S. Kang, S. D. Bu, T. W. Noh, J. Lee, W. Jo, Lanthanum-substituted bismuth titanate for use in non-volatile memories. *Nature* (1999), **401 (6754):** 682-684.

[2] J. S. Kim, S. S. Kim, Ferroelectric properties of Nd-substituted bismuth titanate thin films processed at low temperature. *Appl. Phys. A.* (2005), 81: 1427-1430.

[3] I. W. Kim, C. W. Ahn, J. S. Kim, T. K. Song, J.-S. Bae, B. C. Choi, J.-H. Jeong, J. S. Lee, Low frequency dielectric relaxation and ac conduction of $SrBi_2Ta_2O_9$ thinfilm grown by pulsed laser deposition. *Appl. Phys. Lett.* (2002), **80(21):** 4006-4008.

[4] X. L. Zhong, J. B. Wang, M. Liao, L. Z. Sun, H. B. Shu,C. B. Tan, Y. C. Zhou, Ferroelectric and dielectric properties of Nd^{3+} / Zr^{4+} cosubstituted $Bi_4Ti_3O_{12}$ thin films. *Appl. Phys. Lett.* (2007), **90**: 102906-3.

[5] Y. Shimakawa, Y. Kubo, Y. Tauchi, T. Kamiyama, H.Asano, F. Izumi, Structural distortion and ferroelectric properties of $SrBi_2(Ta_{1-x}Nb_x)_2O_9$. *Appl. Phys. Lett.* (2000), **779(17)**: 2749-2751.

[6] M. M. Kumar, Z.-G. Ye, Dielectric and electrical properties of donor- and acceptor- doped ferroelectric $SrBi_2Ta_2O_9$. J. Appl. Phys. (2001), **90(2):** 934-941.

[7] T. Y. Kim, J. H. Lee, Y. J. Oh, M. R. Choi, H. R. Yoon,W. Jo, H. J. Nam, Local Observation of Ferroelectric $Bi_{3.25}La_{0.75}Ti_3O_{12}$ Thin Films by Atomic Force Microscopy. *J. Korean Phys. Soc.* (2006), **49:** S595- S599.

[8] S.-M. Jung, S.-I. Yoo, Y.-H. Kim, Y. T. Kim, S.-K. Hong, Characteristics of Sol-Gel Derived $Bi_{3.15}Nd_{0.85}Ti_3O_{12}$ Thin Films on Al_2O_3/Si for Metal-Ferroelectric-Insulator-Semiconductor Structure. *J. Korean Phys. Soc.* (2006), **49:** S552- S556.

[9] B. Aurivillius, Ark. Kemi (1951), **1:** 449.

[10] J.F. Scott, A.Carlos and P. De Araujo, *Ferroelectric Memories, Science.* (1989), **246(4936)**: 1400-1405.

[11] A. Ando, M. kimura, Y. Sakabe, Proceedings of the 11th international symposium on application of Ferroelectrics IEEE-UFC (1999), 303-306.

[12] A. Ando, M. kimura, Y. Sakabe, Crystalline structure and piezoelectric properties of Bi layer structured compound $SrBi_2Nb_2O_9$, Extended Abstract of the 9th US-Japan seminar on Dielectric and piezoelectric ceramics. (1999), 115-118.

[13] V. Srivastava, A. K. Jha, R. G. Mendiratta, Dielectric studies of La and Pb doped $SrBi_2Nb_2O_9$ ferroelectric ceramics, *Mat. Lett.* (2006), **60:** 1469–1462.

[14] V. Srivastava, A. K. Jha, R. G. Mendiratta, Structural and electrical studies in La substituted $SrBi_2Nb_2O_9$ ferroelectric ceramics. *Phy B.* (2006), **371:** 337-342.

[15] M. Afqir, A. Tachafine, D. Fasquelle, M. Elaatmani, J.-C. Carru, A. Zegzouti & M. Daoud, Dielectric properties of $SrBi_{1.8}RE_{0.2}Nb_2O_9$ (RE = Yb, Tm, Tb, Gd, Er, Sm and Ce) ceramics. *Solid State Sciences* (2017), **73:** 51–56.

[16] A. Rotaru, A.J. Miller, D.C. Arnold, F.D. Morrison, Towards novel multiferroic and magnetoelectric materials: dipole stability in tetragonal tungsten bronzes. *Philos. Trans. R. Soc. A Math. Phys. Eng. Sci.* (2014). (2009), **372:** 20120451.

[17] G.A. Smolenskii, V.A. Bokov, Coexistence of magnetic and electric ordering in

Crystals. *J. Appl. Phys.* (1964), **35:** 915–918.

[18] T. Katsufuji, M. Masaki, A. Machida, M. Moritomo, K. Kato, E. Nishibori, M. Takata, M. Sakata, K. Ohoyama, K. Kitazawa, H. Takagi, Crystal structure and magnetic properties of hexagonal $RMnO_3$ (R=Y, Lu, and Sc) and the effect of doping, *Phys. Rev. B.* (2002), **66:** 134434: 1-8.

[19] A. Munoz, J. Alonso, M. Martinez-Lopez, M. Cesais, J. Martinez, M. Fernandez-Diaz, Evolution of the magnetic structure of hexagonal $HoMnO_3$ from neutron powder diffraction data, *Chem. Mater.* (2001), **13:** 1497–1505.

[20] M. Afqir, A. Tachafine, D. Fasquelle, M. Elaatmani, J. Carru, A. Zegzouti, M. Daoud, Structure and electric properties of cerium substituted $SrBi_{1.8}Ce_{0.2}Nb_2O_9$ and$SrBi_{1.8}Ce_{0.2}Ta_2O_9$ ceramics, *Process. Appl. Ceram.* (2016), **3:** 183–188.

[21] M. Afqir, A. Tachafine, D. Fasquelle, M. Elaatmani, A. Zegzouti, J.C. Carru, M.

Daoud, Synthesis, structural and dielectric properties of $SrBi_{2-x}Sm_xNb_2O_9$. *Moscow*

Univ. Phys. Bull. (2017), **72:** 196–202.

[22] M. Afqir, A. Tachafine, D. Fasquelle, M. Elaatmani, J. Carru, A. Zegzouti, M. Daoud, Synthesis , structural and dielectric properties of Ho-doped $SrBi_2Nb_2O_9$ prepared by Co-precipitation, *Sci. CHINA Mater.* (2016).

[23] Wu E (1989) POWD, an interactive powder diffraction data interpretation and indexing program, version2.1.School of Physical Sciences, Flinders University of South Australia, Bedford Park, SA 5042, Australia.)

[24] R.D. Shannon, C.T. Prewitt, Effective ionic radii in oxides and flourides, Acta Crystallogr. *Sect. B Struct.Sci.* (1967), **B25:** 925-946.

[25] M. Afqir, A. Tachafine, D. Fasquelle, M. Elaatmani, J.-C. Carru, A. Zegzouti and M. Daoud, Dielectric properties of gadolinium-doped $SrBi_2Nb_2O_9$ ceramics. *Journal of Materials Science: Materials in Electronics.* (2017), **29(2):** 1289–1297.

[26] Y. Wang, J. Wu, Z. Peng, Q. Chen, D. Xin, D. Xiao, J. Zhu, Piezoelectric properties and thermal stability of $Ca_{0.92}(Li,Ce)_{0.04}Bi_2Nb_{2-x}W_xO_9$ high-temperature ceramics. *Appl. Phys. A.* (2015), **119:** 337-341.

[27] V. Shrivastava, A.K. Jha, R.G. Mendiratta, Structural and electrical studies in La substituted SrBi2Nb2O9 ferroelectric ceramics. *Physica B.* (2006), **371:** 337–342.

[28] Y. Shimakawa, H. Imai, H. Kimura, S. Kimura, Y. Kubo, E. Nishibori, M. Takata, M. Sakata, K. Kato, Z. Hiroi, Orbital hybridization and covalency in paraelectric and ferroelectric $SrBi_2Nb_2O_9$. *Phys. Rev. B.* (2002), **66:** 2–6.

[29] I. Coondoo, A. K. Jha, S. K. Aggarwal, Enhancement of dielectric characteristics in donor doped Aurivillius $SrBi_2Ta_2O_9$ ferroelectric ceramics. *Jour.of European Cer. Society* (2007), **27:** 253–260.

[30] P.Goeland, K. L. Yadav, Effect of V^{+5} doping on structural and dielectric properties of $SrBi_2Nb_2O_9$ Synthesized at low temperature, *Physica B.* (2006), **382:** 245–251.

[31] Y. Wu, C. Nguyen, M. J. Forbess, S. Seraj, S. J. Limmer, T. P. Chou, Prossesing and properties of strontium bismuth vandate niobate ferroelectric ceramics, *J. Am. Ceram.* (2001), **84(12):** 2882-2888.

[32] A. Khokhar, P.K. Goyal, O.P. Thakur, K. Sreenivas, Effect of excess of bismuth doping on dielectric and ferroelectric properties of $BaBi_4Ti_4O_{15}$ ceramics. *Ceram. Int.* (2015), 41: 4189-4198.

[33] M. Ajmal, M.U. Islam, G.A. Ashraf, M.A. Nazir, M.I. Ghouri,Physica B (in Press)

[34] M. Adamczyk, Z. Ujma, M. Pawełczyk, Dielectric properties of $BaBi_2Nb_2O_9$ ceramics. *J. Mater. Sci.* (2006), 41: 5317-5322.

[35] I. Coondoo, A. K. Jha, S. K. Agaarwal, Structural, dielectric and electrical studies in tungsten doped $SrBi_2Ta_2O_9$ ferroelectric ceramics. *Ceram.Inter* (2007), 33: 41–47.

[36] G. A. Smolenskii and A. I. Agranovskaya, Dielectric Polarization and Losses of Some Complex Compounds, *Sov.Phys.Tech.Phys.* (1958), **3(3)**: 1380-1389.

[37] P. Victor, R. Ranjith, S.B. krupanidhi, Normal ferroelectric to relaxor behavior in laser ablated Ca-doped barium titanate thin films, *J.Appl.Phys.* (2003), 94(12): 7702-7709.

[38] C.R.Bowen and D.PAlmond, Modelling the 'Universal' Dielectric Response in Heterogeneous Materials Using Microstructural Electrical Networks. *Material Science and Tech.* (2006), 22(6): 719-724.

[39] Y. Noguchi, M. Miyayama, K. Oikawa, T. Kamiyama, M.Osada, M. Kakihana, Defect Engineering for Control of Polarization Properties in $SrBi_2Ta_2O_9$,*Jpn. J. Appl. Phys.* (2002), 41(part1, 11B): 7062-7075.

[40] E.C. Subbarao, A family of ferroelectric bismuth compounds, *J. Phys. Chem. Solids* (1962), 23: 665-676.

[41] C. Long, H. Fan, P. Ren, Structure, Phase Transition Behaviors and Electrical Properties of Nd Substituted Aurivillius Polycrystallines $Na_{0.5}Nd_xBi_{2.5-x}Nb_2O_9$ (x = 0.1, 0.2, 0.3, and 0.5) *Inorg. Chem.* (2013), 52(9): 5045-5054.

[42] C. Long, Q. Chang, Y. Wu, W. He, Y. Li, H. Fan, New layer-structured ferroelectric polycrystalline materials, $Na_{0.5}Nd_xBi_{4.5-x}Ti_4O_{15}$: crystal structures, electrical properties and conduction behaviors. J. Mater. Chem.C (2015), 3(34): 8852-8864.

[43] M. Afqir, A. Tachafine D. Fasquelle M. Elaatmani, Jean-Claude Carru A.- Zegzouti, M. Daoud, Dielectric properties of gadolinium-doped $SrBi_2Nb_2O_9$ ceramics. *J Mater Sci: Mater Electron* (2017), **29(2):** 1289-1297.

[44] Jelena D.Bobic, Mirjana M. Vijatovic Petrovic, Biljana D.Stojanovic 11 - Review of the most common relaxor ferroelectrics and their applications. *Magnetic, Ferroelectric, and Multiferroic Metal Oxides.* (2018), 233-249.

[45] A.A. Bokov, Z.G. Ye, Dielectric relaxation in relaxor ferroelectrics. *J. Adv. Dielectr.* (2012), **2 (2):** 1241010-1241024.

[46] M.D. Gonc¸alves, F.L. Souza, E. Longo, E.R. Leite, E.R. Camargo, Dielectric characterization of microwave sintered lead zirconate titanate ceramics. *Ceram. Int.* (2016), **42:** 14423-14430.

Tables

Due to technical limitations, table 1, 2, 3 and 4 is only available as a download in the Supplemental Files section.

Figures

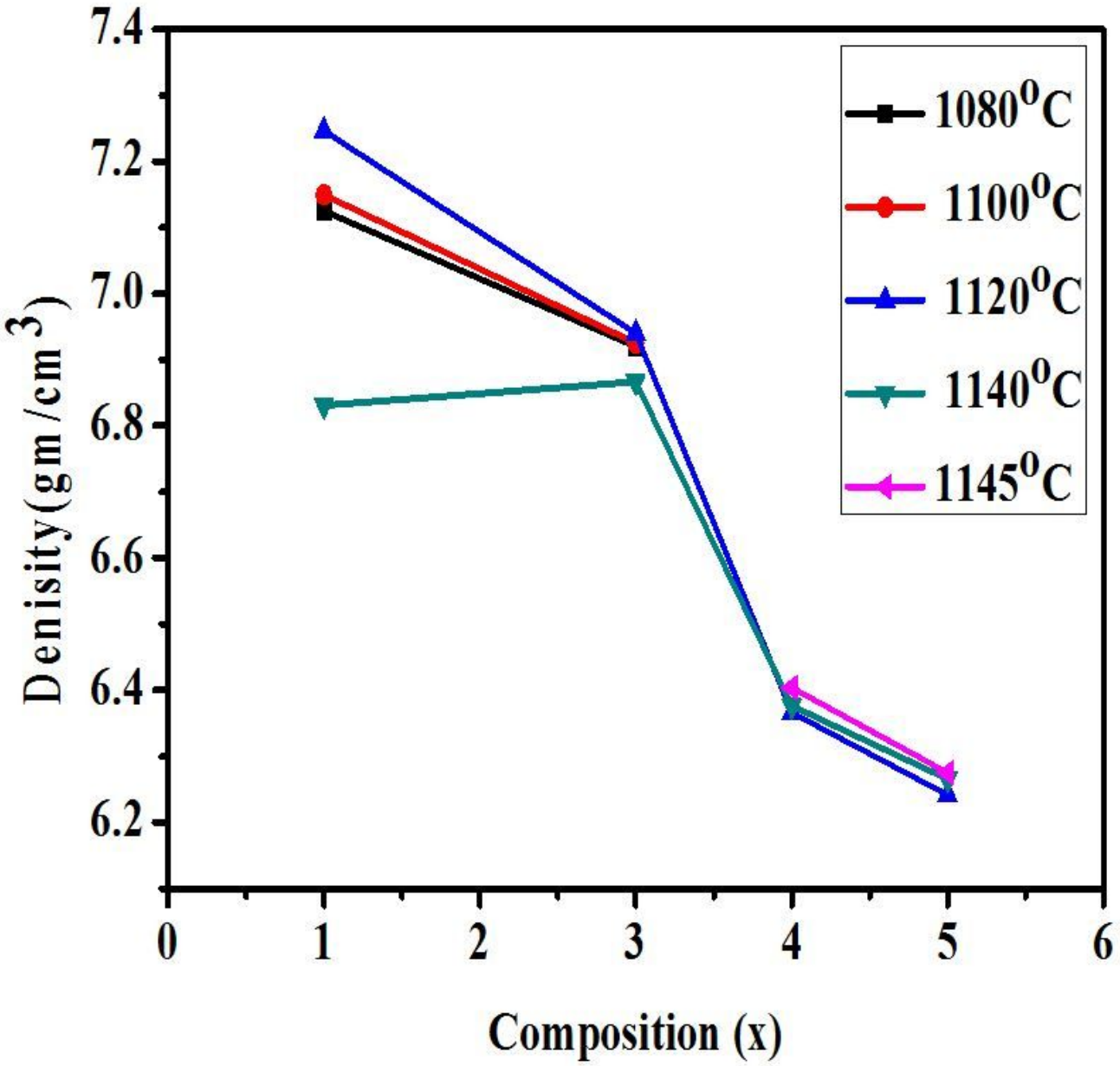

Figure 1

Density versus composition response over the wide temperature range.

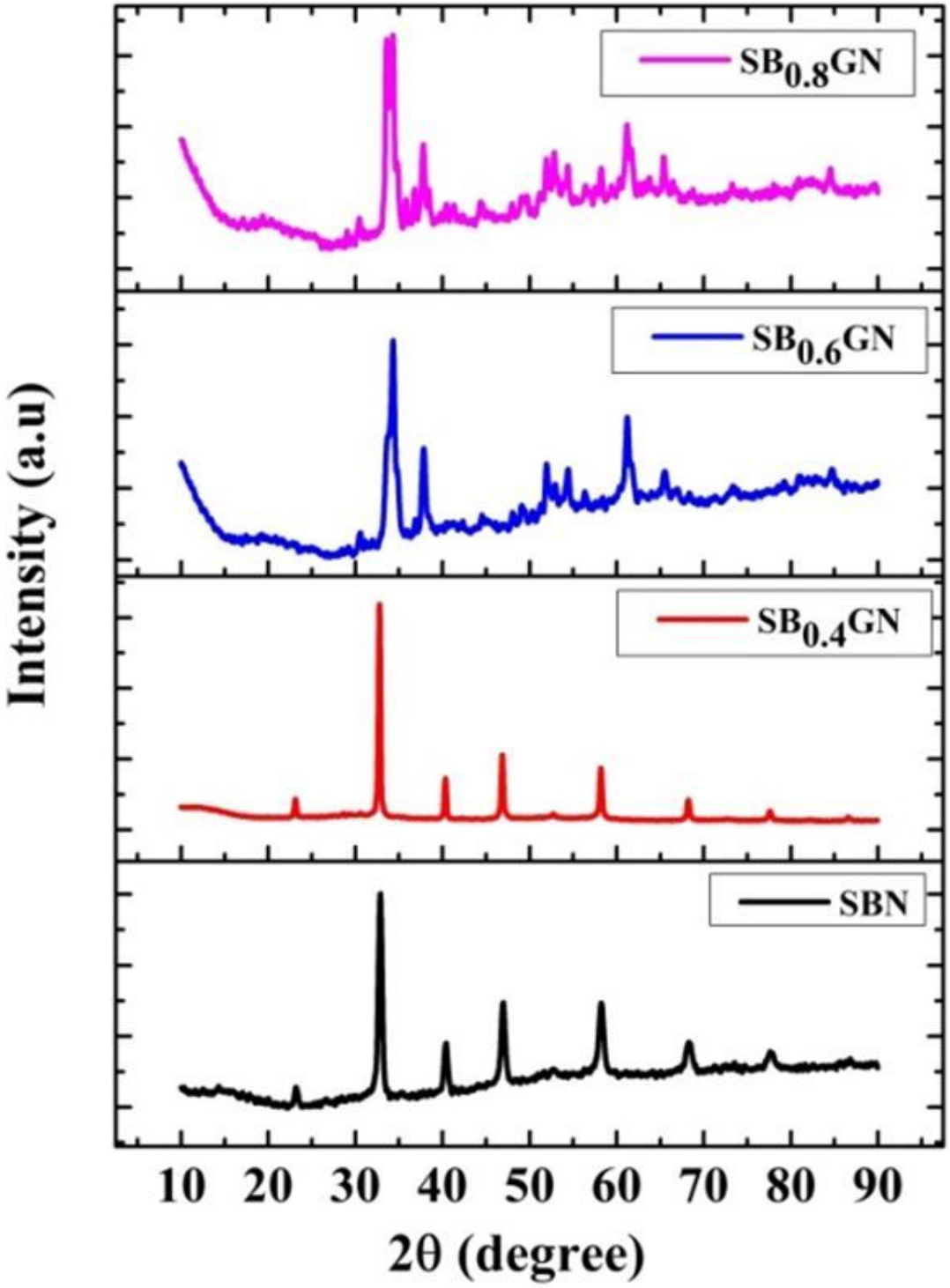

Figure 2

X-Ray diffractograms of SBN and gadolinium modified SBN ceramic powders.

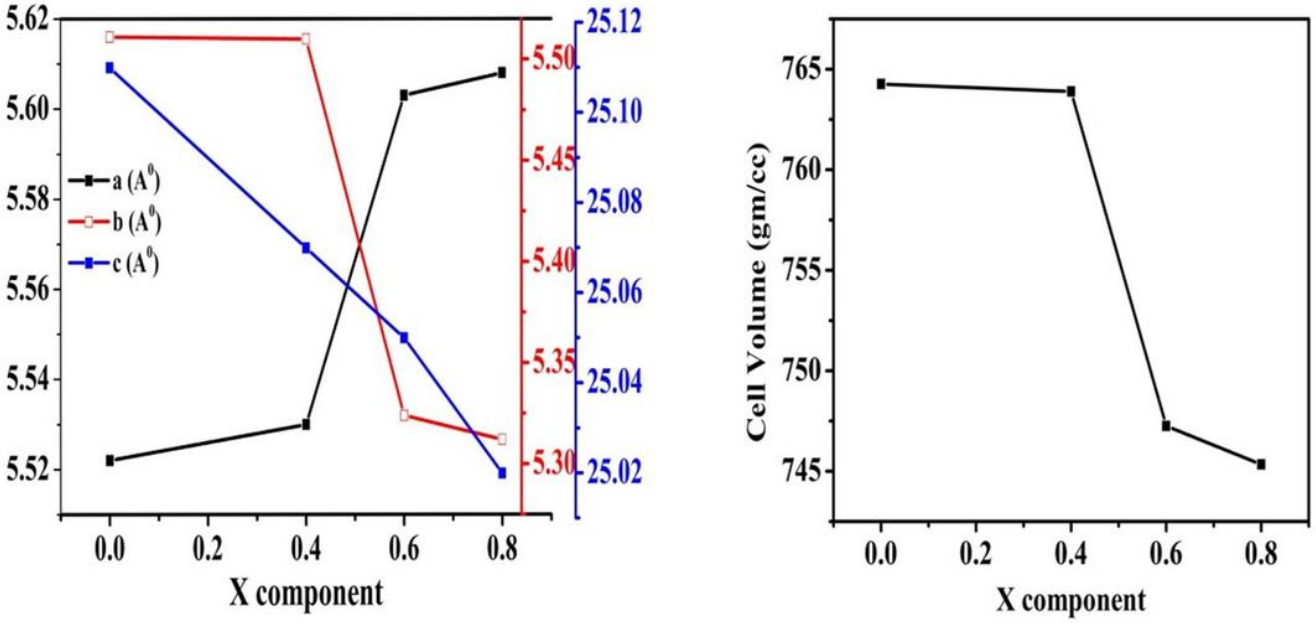

Figure 3

Lattice parameters and Cell volume as a function of X content in SrBi2-xGdxNb2O9 (x = 0.0, 0.4, 0.6 and 0.8) ceramic powders.

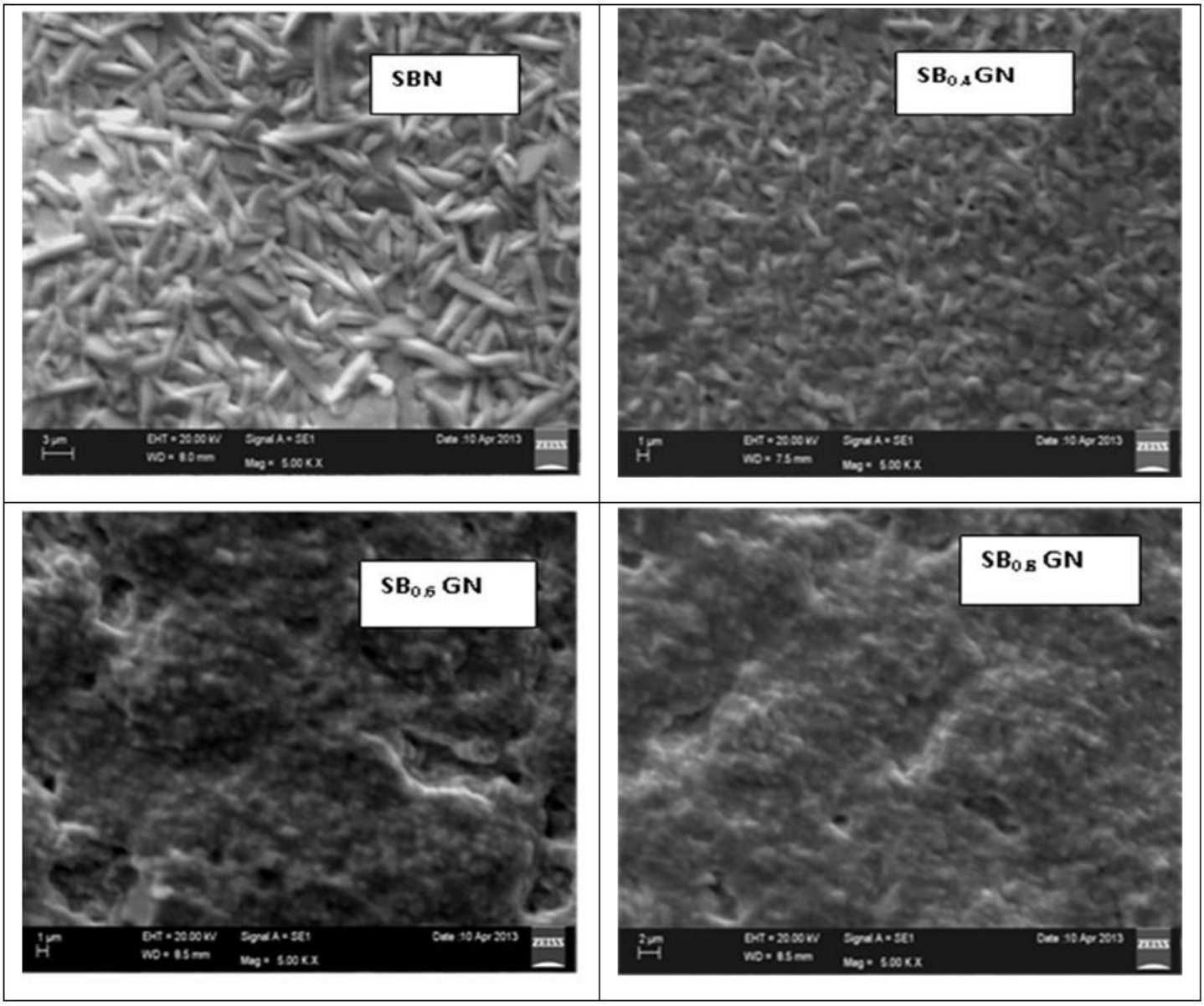

Figure 4

SEM images of SBN and gadolinium doped SrBi2-xGdxNb2O9 (x = 0.4, 0.6 and 0.8) ceramics.

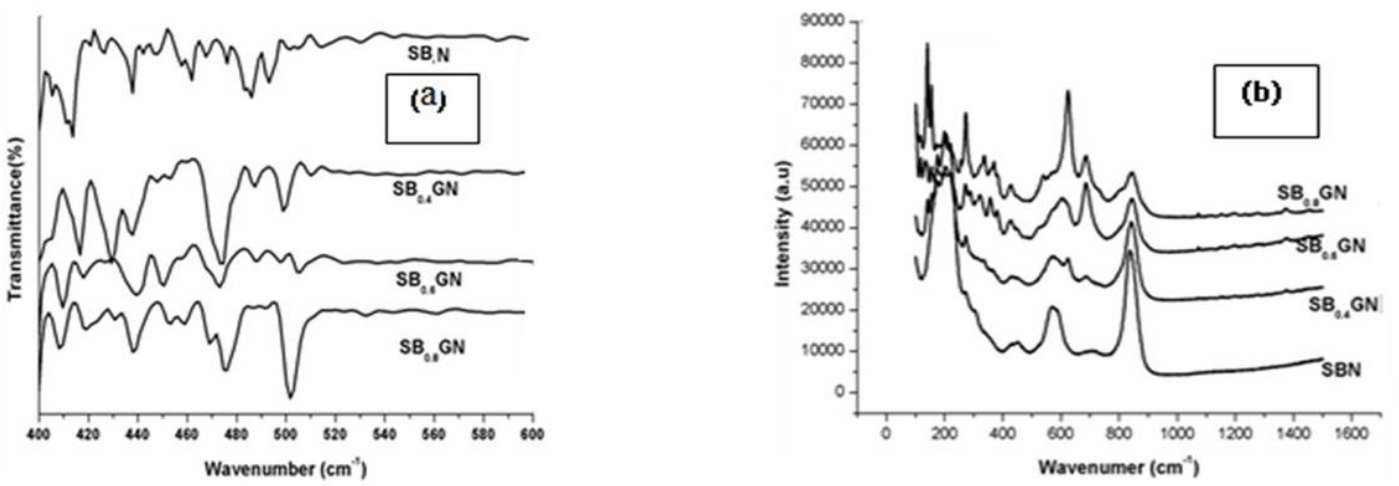

Figure 5

FTIR and RAMAN spectra of SrBi2-xGdxNb2O9 (x =0.0, 0.4, 0.6 and 0.8) ceramic powders.

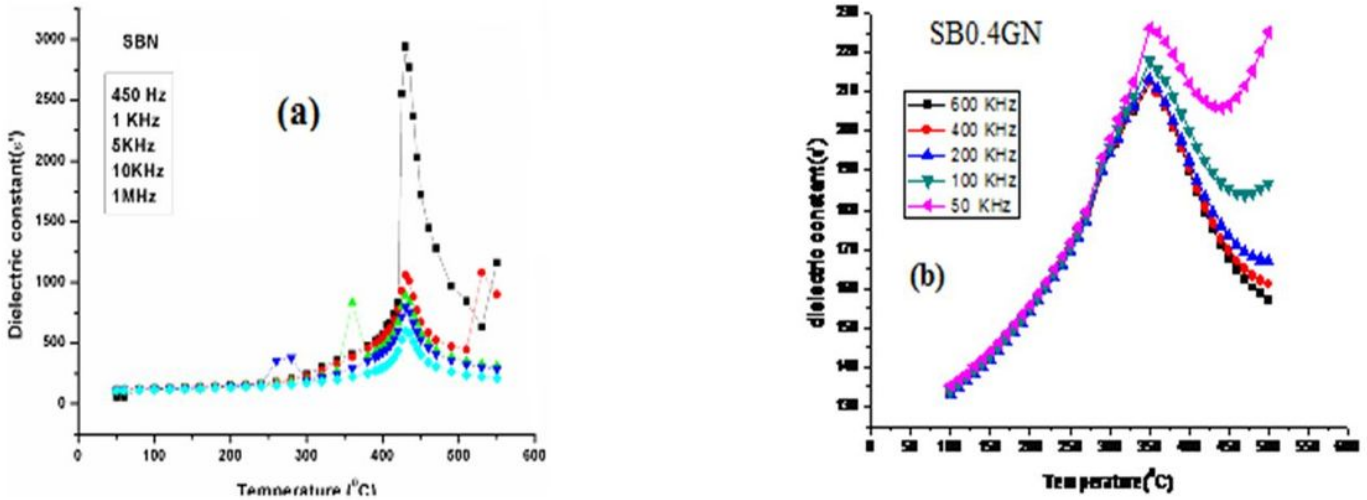

Figure 6

Dielectric permittivity as a function of temperature at different frequencies of SBN and SB0.4GN ceramic materials.

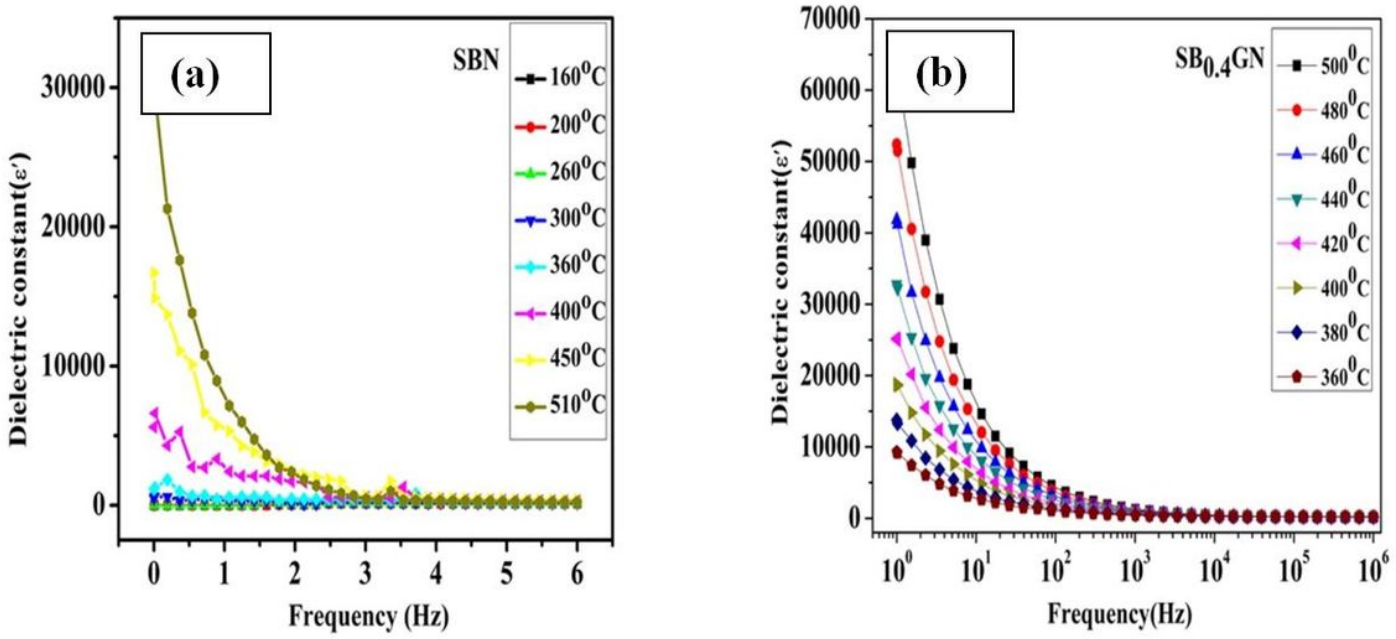

Figure 7

Frequency dependent of dielectric permittivity at different temperatures of SBN and Gadolinium doped SBN ceramics.

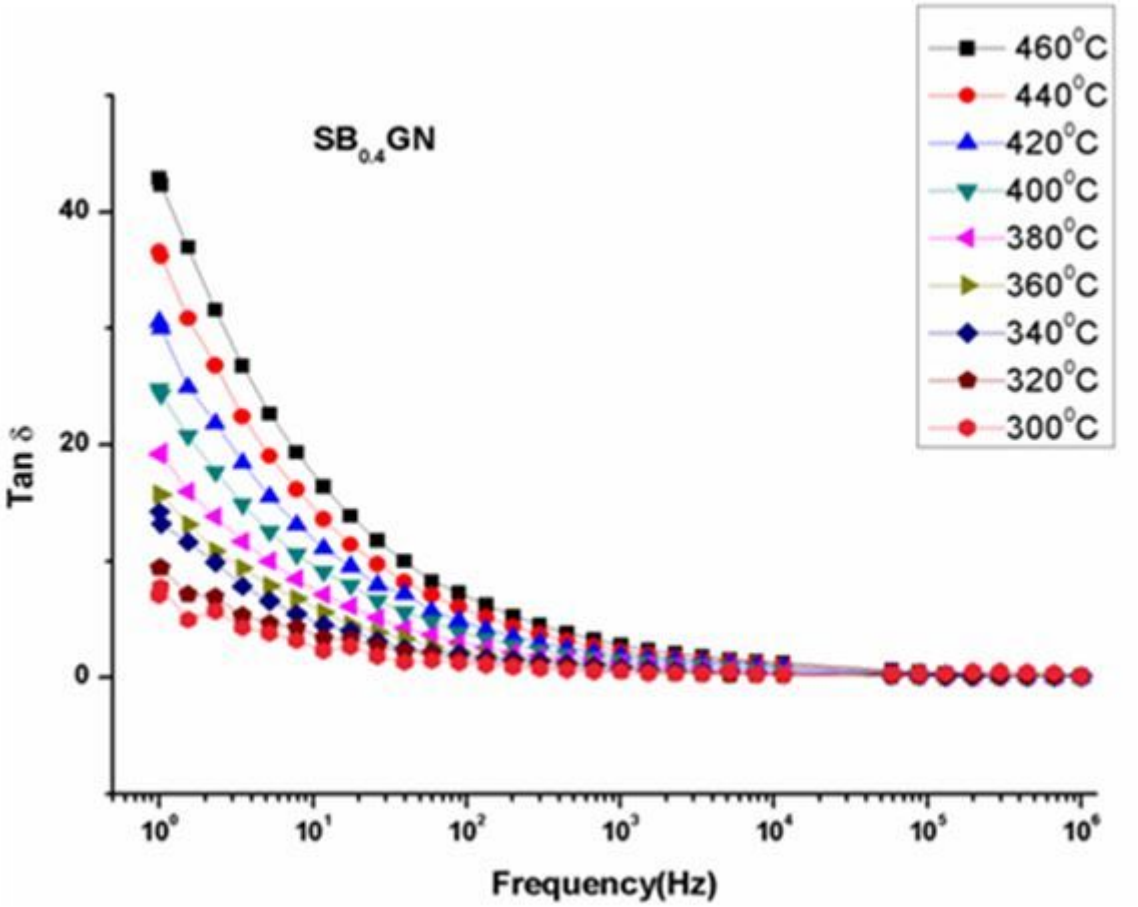

Figure 8

dielectric loss as a function of frequency at different temperatures of SB0.4GN ceramic material.

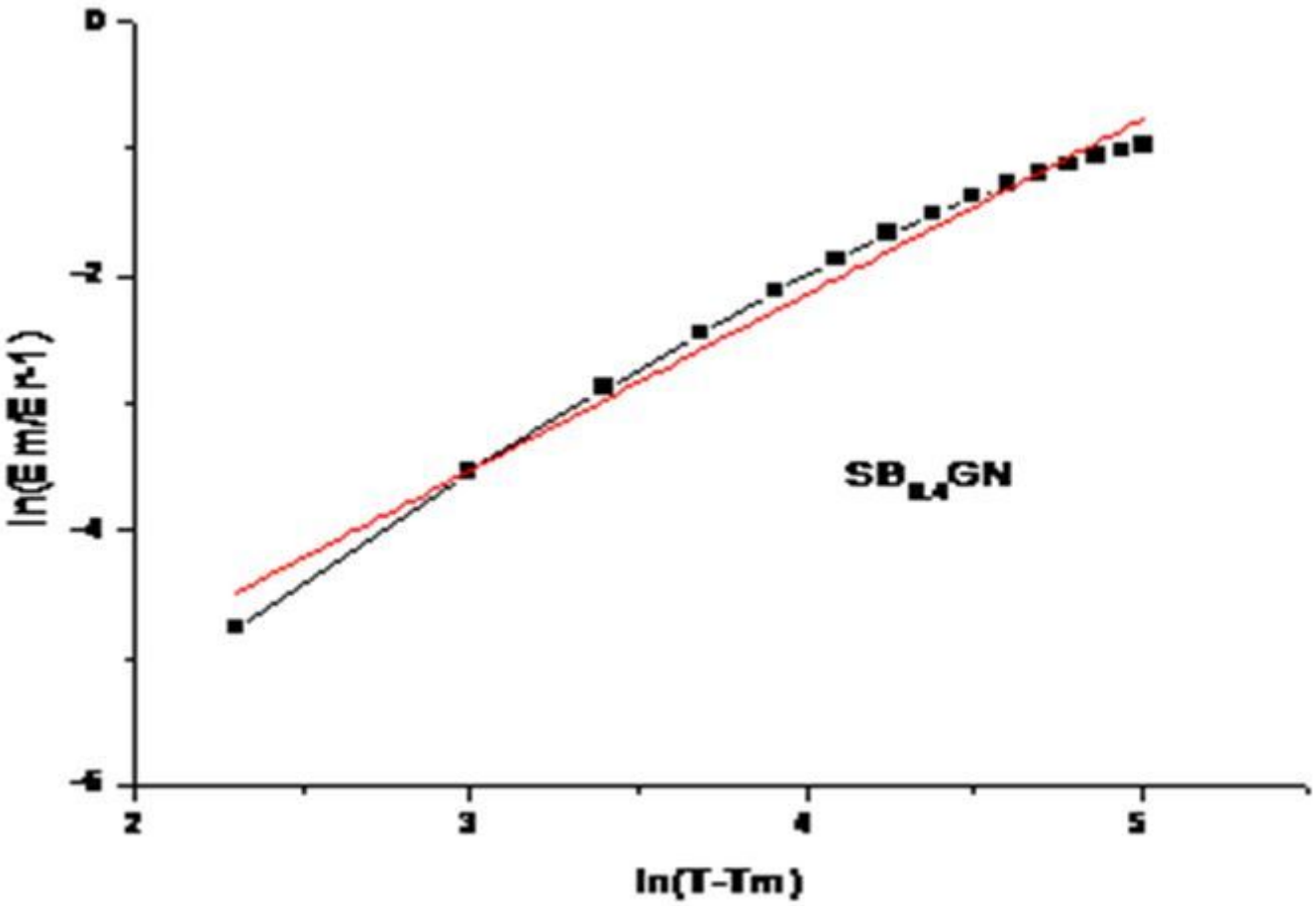

Figure 9

ln(1/ε' − 1/ε'm) as a function of ln(T − Tm) at 1 MHz of Gd doped SrBi2Nb2O9 ceramics.

Supplementary Files

This is a list of supplementary files associated with this preprint. Click to download.

- TablesofSBGN1JAC.docx